Radiation and Mass Transfer Effects on MHD Flow of a Micropolar Fluid towards a Stagnation Point on a Vertical Stretching Sheet

E. Manjoolatha, N. Bhaskar Reddy and T.Poornima

Department of Mathematics, Sri Venkateswara University, Tirupati - 517502, A.P.

ABSTRACT

This paper focuses on the study of magnetohydrodynamic mixed convection flow of a micropolar fluid near a stagnation point on a vertical stretching sheet in the presence of radiation and mass transfer. Using the similarity transformations, the governing equations have been transformed into a system of ordinary differential equations. The resultant dimensionless governing equations are solved employing fourth order Runge-Kutta method along with shooting technique. The effects of various governing parameters, namely, material parameter, radiation parameter, magnetic parameter and velocity ratio parameter on the velocity, microrotation, temperature and concentration, as well as the skin friction, the rate of heat transfer and the rate of mass transfer have been computed and shown graphically. It is observed that the micropolar fluid helps in the reduction of drag forces and also act as a cooling agent.

Keywords - Micropolar fluid, Mixed convection, Stagnation point, Stretching sheet, Radiation, Mass transfer, MHD .

1. INTRODUCTION

In recent years, the dynamics of micropolar fluids, originating from the theory of Eringen [1], has been a popular area of research. This theory takes into account the effect of local rotary inertia and couple stresses arising from practical microrotation action. This theory is applied to suspensions, liquid crystals, polymeric fluids and turbulence. This behavior is familiar in many engineering and physical applications. Also, the study of boundary layer flows of micropolar fluids over a stretching surface has received much attention because of their extensive applications in the field of metallurgy and chemical engineering for example, in the extrusion of polymer sheet from a die or in the drawing of plastic films. Na and Pop [2] investigated the boundary layer flow of a micropolar fluid past a stretching wall. Desseaux and Kelson [3] studied the flow of a micropolar fluid bounded by a stretching sheet. Hady [4] studied the solution of heat transfer to micropolar fluid from a non-isothermal stretching sheet with injection. However, of late, the effects of a

magnetic field on the micropolar fluid problem are very important.

The problem of stretching sheet under the influence of magnetic field is also an interesting problem of research. Such investigations of MHD flows are industrially important and have applications in different areas of research such as petroleum production, geophysical flows, cooling of underground electric cables etc. It has been found that the application of a magnetic field reduces the heat transfer at the stagnation point and increases the skin friction. These features are useful in the design of heat shield for protecting the spacecraft entering or re-entering the atmosphere. Abo-Eldahaband Ghonaim [5] investigated convective heat transfer in an electrically conducting micropolar fluid at a stretching surface with uniform free stream. Mohammadein and Gorla [6] investigated the transverse magnetic field on mixed convection in a micropolar fluid flowing on a horizontal plate with vectored mass transfer. They analyzed the effects of a magnetic field with vectored surface mass transfer and induced buoyancy stream wise pressure gradients on heat transfer. Bhargava et al. [7] studied the numerical solution of the problem of free convection micropolar fluid flow between two parallel porous vertical plates in the presence of magnetic field. Srinivasacharya and Shiferaw [8] presented numerical solution of the steady conducting micropolar fluid through porous annulus under the influence of an applied uniform magnetic field. Rawat et el. [9] investigated the steady, laminar free convection flow of an electrically-conducting fluid between two vertical plates embedded in a non-Darcy porous medium in the presence of uniform magnetic field with heat generation/absorption and variable thermal conductivity effects.

Stagnation flow, fluid motion near the stagnation region, exists on all solid bodies moving in a fluid. Problems such as the extrusion of polymers in melt-spinning processes, glass blowing, the continuous casting of metals, and the spinning of fibers all involve some aspect of flow over a stretching sheet or cylindrical fiber by Paullet and weidman [10]. Ishak et al. [11] theoretically studied the similarity solutions for the steady magnetohydrodynamic flow towards a

stagnation point on a vertical surface immersed in an incompressible micropolar fluid. Lokendra Kumar [12] has analyzed the effect of MHD flow of micropolar fluid towards a stagnation point on a vertical stretching sheet. Ishak et al. [13] investigated the steady two-dimensional stagnation point flow of an incompressible micropolar fluid towards a vertical stretching sheet.

Due to recent advances in space technology and nuclear energy the study of natural convection still continues to be a major area of interest. The natural convection in fluids with microstructure has been an important area of research. Flows in which buoyancy forces are dominant are called natural and the respective heat transfer being known as natural convection. This occurs at very small velocity of motion in the presence of large temperature differences. These temperature differences cause density gradients in the fluid medium and in the presence of gravitational body force, free convection effects become important. In forced convection case, the natural convection effects are also present because of the presence of gravitational body force. A situation where both the natural and forced convection effects are of comparable order is known as mixed or combined convection.

The study of mixed convection is very important in view of several physical problems. In several practical applications, there exist significant temperature differences between the surface of the body and the free stream. In such flows the flow and thermal fields are no longer symmetric with respect to stagnation line. The friction factor and local heat transfer rate can be quite different under these conditions related to the forced convection case. Ishak et al [14] studied mixed convection stagnation point flow of a micropolar fluid towards a stretching surface. Hassanien and Gorla [15] have considered the mixed convection in stagnation flows of micropolar fluids with an arbitrary variation of surface temperature. The problem of unsteady mixed convection in two dimensional stagnation flows of micropolar fluids on a vertical flat plate when the plate temperature varies linearly with the distance along the plate has been considered by Lok et al. [16]. Bhargava et al. [17] analyzed the effect of surface conditions on the mixed convection micropolar flow driven by a porous stretching sheet.

In the context of space technology and in the processes involving high temperatures, the effects of radiation are of vital importance. Recent developments in hypersonic flights, missile re-entry, rocket combustion chambers, power plants for inter planetary flight and gas cooled nuclear reactors, have focused attention on thermal radiation as a mode of energy transfer, and emphasized the need for improved understanding of radiative transfer in these processes. Ogulu [18]

studied the oscillating plate-temperature flow of a polar fluid past a vertical porous plate in the presence of couple stresses and radiation. Rahman and Sattar [19] studied transient convective heat transfer flow of a micropolar fluid past a continuously moving vertical porous plate with time dependent suction in the presence of radiation. Abd-El Aziz and Cairohave [20] analyzed the thermal radiation effects on magnetohydrodynamic mixed convection flow of a micropolar fluid past a continuously moving semi-infinite plate for high temperature differences. Rahman and Sultana [21] discussed the radiative heat transfer flow of micropolar fluid with variable heat flux in a porous medium.

Many transport processes exist in nature and in industrial applications in which the simultaneous heat and mass transfer occur as a result of combined buoyancy effects of thermal diffusion and diffusion of chemical species. A few representative fields of interest in which combined heat and mass transfer plays an important role are designing of chemical processing equipment, formation and dispersion of fog, distribution of temperature and moisture over agricultural fields and groves of fruit trees, crop damage due to freezing, and environmental pollution. In this context, Callahan and Marner [22] considered the transient free convection flow past a semi-infinite vertical plate with mass transfer. Unsteady free convective flow on taking into account the mass transfer phenomenon past an infinite vertical plate was studied by Soundalgekar and Wavre[23]. Kumar [24] analyzed the effect of heat and mass transfer in the hydromagnetic micropolar fluid flow along a stretching sheet. Bhargava et al. [25] studied coupled fluid flow, heat and mass transfer phenomena of micropolar fluids over a stretching sheet with non-linear velocity.

The aim of the present study is to analyze the effects of magnetohydrodynamic mixed convection flow of a micropolar fluid near a stagnation point on a vertical stretching sheet by taking the radiation and mass transfer into account. Using the similarity transformations, the governing equations have been transformed into a set of ordinary differential equations, and the resultant equations are solved using Runge-Kutta method along with shooting technique. The behavior of the velocity, microrotation, temperature and concentration, as well as the skin friction, the rate of heat transfer and the rate of mass transfer for variations in the thermo-physical parameters, namely, material parameter, magnetic parameter, radiation parameter and velocity ratio parameter have been computed and discussed in detail.

2. MATHEMATICAL FORMULATION

A steady, two-dimensional flow of an incompressible, electrically conducting micropolar

fluid near a stagnation point on a vertical heated stretching sheet is considered. The x-axis is taken along the sheet and y-axis normal to it. The fluid occupies the half plane (y>0). It is assumed that the velocity of the flow external to the boundary layer $u_e(x)$, velocity of the stretching sheet $u_w(x)$, the temperature of the sheet $T_w(x)$ and concentration of sheet are proportional to the distance x from the stagnation point, i.e. $u_e(x) = ax, u_w(x) = cx$, $T_w(x) = T_\infty + bx$ and $C_w(x) = C_\infty + dx$, where a, b, c and d are constants, $T_w(x) > T_\infty$ with T_∞ being the uniform temperature of the fluid and $C_w(x) > C_\infty$ with C_∞ being the uniform concentration of the fluid. A uniform magnetic field of strength B_0 is assumed to be applied in the positive y-direction normal to the plate. The magnetic Reynolds number of the flow is taken to be small enough so that the induced magnetic field is negligible. The level of concentration of foreign mass is assumed to be low, so that the Soret and Dufour effects are negligible. Under the usual boundary layer approximation, the governing equations are

$$\frac{\partial u}{\partial x} + \frac{\partial v}{\partial y} = 0 \qquad (2.1)$$

$$u\frac{\partial u}{\partial x} + v\frac{\partial u}{\partial y} = u_e\frac{du_e}{dx} + \left(\frac{\mu+\kappa}{\rho}\right)\frac{\partial^2 u}{\partial y^2} + \frac{\kappa}{\rho}\frac{\partial N}{\partial y}$$
$$- \frac{\sigma B_0^2}{\rho}(u_e - u) \pm g\beta_T(T - T_\infty) \pm g\beta_C(C - C_\infty)$$
$$(2.2)$$

$$\rho j\left(u\frac{\partial N}{\partial x} + v\frac{\partial N}{\partial y}\right) = \gamma\frac{\partial^2 N}{\partial y^2} - \kappa\left(2N + \frac{\partial u}{\partial y}\right)$$
$$(2.3)$$

$$u\frac{\partial T}{\partial x} + v\frac{\partial T}{\partial y} = \alpha\frac{\partial^2 T}{\partial y^2} - \frac{\alpha}{k}\frac{\partial q_r}{\partial y} \qquad (2.4)$$

$$u\frac{\partial C}{\partial x} + v\frac{\partial C}{\partial y} = D\frac{\partial^2 C}{\partial y^2} \qquad (2.5)$$

The boundary conditions for the velocity, temperature and concentration fields are

$$u = u_w(x), v = 0, N = -\frac{1}{2}\frac{\partial u}{\partial y}, T = T_w(x), C = C_w(x) \text{ at}$$
$$y = 0$$
$$u \to u_e(x), N \to 0, T \to T_\infty, C \to C_\infty \text{ as}$$
$$y \to \infty$$
$$(2.6)$$

where u and v are the velocity components along the x and y axes, respectively, g - the acceleration due to gravity, T - the fluid temperature in the boundary layer and C - the fluid concentration in the boundary layer, υ -the kinematic viscosity, β_T - the thermal expansion coefficient, β_C - the coefficient of expansion with concentration, B_0 - the magnetic field of constant strength, q_r - the radiative heat flux, D - the coefficient of mass diffusivity. Further, μ, κ, ρ, j, N, γ, α and k are respectively the dynamic viscosity, vortex viscosity (or the microrotation viscosity), fluid density, micro-inertia density, microrotation vector (or angular velocity), spin gradient viscosity, thermal diffusivity and thermal conductivity.

Following the work of many authors, we assume that γ = (μ +κ/ 2) j = μ (1+ K/ 2) j, where K =κ /μ is the material parameter. This assumption is invoked to allow the field of equations predicts the correct behavior in the limiting case when the microstructure effects become negligible and the total spin N reduces to the angular velocity. The last terms on the right-hand side of (2.2) represents the influence of the thermal and solutal buoyancy forces on the flow field and ' $\pm$ ' indicates the buoyancy assisting and the opposing the flow regions, respectively.

By using the Rosseland approximation (Brewster [26]), the radiative heat flux q_r is given by

$$q_r = -\frac{4\sigma^*}{3K'}\frac{\partial T^4}{\partial y} \qquad (2.7)$$

where σ^* is the Stefan-Boltzmann constant and K' - the mean absorption coefficient. It should be noted that by using the Rosseland approximation, the present analysis is limited to optically thick fluids. If temperature differences within the flow are sufficiently small, then equation (2.7) can be linearized by expanding T^4 into the Taylor series about T_∞, which after neglecting higher order terms takes the form

$$T^4 \cong 4T_\infty^3 T - 3T_\infty^4 \qquad (2.8)$$

In view of equations (2.7) and (2.8), equation (2.4) reduces to

$$u\frac{\partial T}{\partial x} + v\frac{\partial T}{\partial y} = \alpha\left(1 + \frac{16\sigma^* T_\infty^3}{3K'k}\right)\frac{\partial^2 T}{\partial y^2} \qquad (2.9)$$

The continuity equation (2.1) is satisfied by the Cauchy Riemann equations

$$u = \frac{\partial \psi}{\partial y} \text{ and } v = -\frac{\partial \psi}{\partial x} \qquad (2.10)$$

where $\psi(x, y)$ is the stream function.

In order to transform equations (2.2), (2.3), (2.9) and (2.5) into a set of ordinary differential equations, the following similarity transformations and dimensionless variables are introduced.

$$f(\eta) = \frac{\psi}{(c\upsilon)^{1/2} x}, \ \eta = y\sqrt{\frac{c}{\upsilon}},$$

$$h(\eta) = \frac{N}{c(c\upsilon)^{1/2} x}, \ j = \frac{\upsilon}{c}, \theta(\eta) = \frac{T - T_\infty}{T_w - T_\infty},$$

$$\phi(\eta) = \frac{C - C_\infty}{C_w - C_\infty}, \quad M = \frac{\sigma B_0^2}{\rho c}, \quad \lambda = \frac{Gr}{\mathrm{Re}_x^2},$$

$$Gr = \frac{g\beta_T (T_w - T_\infty)x^3}{\upsilon^2},$$

$$Gc = \frac{g\beta_C (C_w - C_\infty)x^3}{\upsilon^2}, \delta = \frac{Gc}{\mathrm{Re}_x^2}, \mathrm{Pr} = \frac{\upsilon}{\alpha},$$

$$Sc = \frac{\upsilon}{D}, R = \frac{K'k}{4\sigma * T_\infty^3}, \mathrm{Re}_x = \frac{u_e x}{\upsilon}$$

(2.11)

where $f(\eta)$ is the dimensionless stream function, θ is the dimensionless temperature, ϕ is the dimensionless concentration, η is the similarity variable, j is the characteristic length, M is the magnetic parameter, Gr is the local thermal Grashof number, Gc is the local solutal Grashof number, Pr is the Prandtl number, λ is the thermal buoyancy parameter, δ is the solutal buoyancy parameter, Sc is the Schmidt number and R is the radiation parameter.

In view of equations (2.10) and (2.11), the equations (2.2), (2.3), (2.9) and (2.5) transform into

$$(1+K)f''' + ff'' + \left(\frac{a}{c}\right)^2 - f'^2 + Kh' + M\left(\frac{a}{c} - f'\right) \pm \lambda\theta \pm \delta\phi = 0$$

(2.12)

$$(1 + K/2)h'' + fh' - f'h - K(2h + f'') = 0$$

(2.13)

$$\left(\frac{1+R}{\mathrm{Pr}\,R}\right)\theta'' + f\theta' - f'\theta = 0$$

(2.14)

$$\phi'' + Scf\phi' - Scf'\phi = 0$$

(2.15)

The corresponding boundary conditions are

$$f = 0, f' = 1, h = -\frac{1}{2}f'', \theta = 1, \phi = 1 \text{ at } \eta = 0$$

$$f' = \frac{a}{c}, h = \theta = \phi = 0. \text{ as } \eta \to \infty \quad (2.16)$$

where the primes denote differentiation with respect to η

The physical quantities of interest are the skin friction coefficient C_f, the local Nusselt number Nu and Sherwood number Sh which are defined as

$$C_f = \frac{\tau_w}{\rho u_w^2 / 2}, \qquad Nu = \frac{xq_w}{k(T_w - T_\infty)},$$

$$Sh = \frac{xM_n}{D(C_w - C_\infty)}$$

where k is the thermal conductivity and, the wall shear stress τ_w, the heat flux q_w and mass flux M_n are given by

$$\tau_w = \left[(\mu + \kappa)\frac{\partial u}{\partial y} + \kappa N\right]_{y=0},$$

$$q_w = -k\left(\frac{\partial T}{\partial y}\right)_{y=0} \qquad M_n = -D\left(\frac{\partial C}{\partial y}\right)_{y=0}$$

Using the similarity variables (2.11), we obtain

$$\frac{1}{2}C_f \mathrm{Re}_x^{1/2} = \left(1 + \frac{K}{2}\right)f''(0),$$

$$Nu / \mathrm{Re}_x^{1/2} = -\theta'(0), \ Sh / \mathrm{Re}_x^{1/2} = -\phi'(0)$$

Our main aim is to investigate how the values of $f''(0)$, $-\theta'(0)$ and $-\phi'(0)$ vary in terms of the radiation and buoyancy parameters.

3 SOLUTION OF THE PROBLEM

The set of coupled non-linear governing boundary layer equations (2.12) - (2.15) together with the boundary conditions (2.16) are solved numerically using Runge-Kutta method along with shooting technique. First of all, higher order non-linear differential equations (2.12) - (2.15) are converted into simultaneous linear differential equations of first order and they are further transformed into initial value problem by applying the shooting technique (Jain *et al.*[27]). The resultant initial value problem is solved by employing Runge-Kutta fourth order method. The step size $\Delta\eta = 0.05$ is used to obtain the numerical solution with five decimal place accuracy as the criterion of convergence. From the process of numerical computation, the skin-friction coefficient, the Nusselt number and the Sherwood number, which are respectively proportional to $f''(0), -\theta'(0)$ and $-\phi'(0)$, are also sorted out and their numerical values are presented in graphs.

4 RESULTS AND DISCUSSION

In order to get a physical insight of the problem, a representative set of numerical results is shown graphically in Figures 1-16, to illustrate the influence of physical parameters viz., material parameter, magnetic parameter, radiation parameter and velocity ratio parameter on the velocity, microrotation, temperature and concentration as

well as the skin-friction coefficient, Nusselt number and Sherwood number for both the cases of assisting and opposing flows. Throughout the computations, the Prandtl number and Schmidt number are taken to be 0.71 and 0.22(unless otherwise stated).

Fig.1 illustrates the velocity profiles for different values of the magnetic parameter M. It is observed that the velocity decreases with an increase in the magnetic parameter for assisting flow, whereas it increases for opposing flow. Maximum for assisting flow and minimum for opposing flow shift away from the wall with an increase in the magnetic parameter. Thus the fluid flow can be effectively controlled by introducing the magnetic field to the Newtonian fluid. From Fig.2, it is noticed that as the magnetic parameter increases, the microrotation increases for assisting flow while it decreases for opposing flow. It is also clear that for opposing flow the microrotation becomes negative away from the boundary which shows the reverse rotation. For assisting flow the microrotation is negative near the boundary.

Fig.3 represents the temperature distribution with the variation of magnetic parameter M. For assisting flow it increases with an increase in magnetic parameter, while a reverse pattern is observed for opposing flow. Fig.4 depicts the concentration distribution with the variation of magnetic parameter. For assisting flow it increases with an increase in magnetic parameter, while a reverse pattern is observed for opposing flow. Thus the high temperature or the high concentration can be controlled by magnetic parameter or the buoyancy parameters, which is required in many engineering applications.

Fig.5 depicts the velocity profiles for different values of the material parameter (K), for both assisting and opposing flows. It is observed that the velocity decreases with an increase in the material parameter (K) for assisting flow whereas it increases for opposing flow. Maximum for assisting flow and minimum for opposing flow shift away from the wall with increasing material parameter. Thus the fluid flow can be effectively controlled by introducing micro-constituents to the Newtonian fluid.

Fig.6 shows the microrotation distribution with the variation of material parameter. For assisting flow the microrotation decreases with an increase in the material parameter while it increases for opposing flow. It is clear from the figure that for opposing flow the microrotation becomes negative near the boundary. For assisting flow the microrotation is negative away from the boundary which shows the reverse rotation. The temperature distribution with the variation of material parameter is shown in Fig.7. It has been observed that for assisting flow the temperature increases with the increase in the material parameter while it

decreases for opposing flow. The concentration distribution with the variation of material parameter is shown in Fig.8. It has been observed that for assisting flow the concentration increases with the increase in the material parameter while for opposing flow it decreases. Thus the temperature and concentration can be controlled by the material parameter. The desired temperature or the concentration can be generated by controlling the buoyancy parameters or the material parameter.

The distribution for the velocity with the velocity ratio parameter a/c has been displayed in Fig.9. The value of $a/c>1$ shows that the stretching velocity is less than the free stream velocity while value $a/c<1$ shows that the stretching velocity is greater than the free stream velocity. It is observed that the velocity increases with an increase in the velocity ratio parameter. Thus the fluid flow can be effectively controlled by controlling a/c. Near the boundary it is observed that the velocity is higher for assisting flow as compared to the opposing flow. The microrotation profiles for the variation of velocity ratio parameter a/c are shown in Fig.10. Clearly the angular rotation decreases with an increase in a/c for both assisting and opposing flows. It is obvious from the figure that for opposing flow microrotation is higher than those for assisting flow. For large values of a/c, microrotation becomes negative which shows the reverse rotation.

The temperature profiles for the variation of velocity ratio parameter a/c are presented in Fig.11. Temperature decreases with an increase in a/c for both assisting and opposing flows. It is clear from the figure that the temperature is higher for opposing flow when compared with the temperature for assisting flow. The concentration profiles for the variation of velocity ratio parameter a/c are presented in Fig.12. Concentration decreases with an increase in a/c for both assisting and opposing flows. It is clear from the figure that the concentration is higher for opposing flow when compared with the concentration for assisting flow. Thus the temperature or the concentration can be effectively controlled by increasing or decreasing the stretching or the free stream velocities.

Fig.13 depicts the velocity profiles for different values of the radiation parameter R, for both assisting and opposing flows. It is observed that the velocity decreases with an increase in the radiation parameter for assisting flow whereas it increases for opposing flow. Maximum for assisting flow and minimum for opposing flow shift away from the wall with increasing radiation parameter. Fig.14 shows the microrotation distribution with the variation of radiation parameter. For assisting flow the microrotation increases with an increase in the radiation parameter, while it decreases for opposing flow. It is clear from the figure that for opposing flow the

microrotation becomes negative away from the boundary which shows the reverse rotation. For assisting flow the microrotation is negative near the boundary.

The temperature profiles with the variation of radiation parameter are presented in Fig.15. Temperature decreases with an increase in the radiation parameter for both assisting and opposing flows. It is clear from the figure that the temperature is higher for opposing flow when compared with the temperature for assisting flow. Thus the temperature can be effectively controlled by the radiation parameter.The concentration profiles for the variation of the radiation parameter are presented in Fig.16. Concentration increases with an increase in the radiation parameter for both assisting and opposing flows. It is clear from the figure that the concentration is higher for opposing flow when compared with the concentration for assisting flow.

The skin friction, rate of heat transfer and rate of mass transfer with the buoyancy parameter λ for different values of the radiation parameter R, are shown graphically in Figs. 17-19. From Fig.17, it is observed that for opposing flow the skin friction increases with the increase of the radiation parameter while reverse pattern is observed for assisting flow. From Fig.18, it is noticed that the Nusselt number increases with the increase of the radiation parameter for both assisting and opposing flows. From Fig.19, it is observed that for opposing flow the Sherwood number decreases with the increase of the radiation parameter while reverse pattern is observed for assisting flow.

5 CONCLUSIONS

An attempt is made to study the effects of radiation and mass transfer on MHD mixed convection flow of a micropolar fluid near a stagnation point on a vertical stretching sheet. The governing equations are approximated to a system of non-linear ordinary differential equations by similarity transformation. The behavior of the velocity, microrotation, temperature and concentration as well as the skin friction, Nusselt number and Sherwood number are shown graphically for various values of the governing parameters. In the buoyancy-assisting flow region, the skin friction decreases with increasing values of the radiation parameter, whereas, the opposite behavior is observed in the buoyancy-opposing flow region. For both assisting and opposing flows the rate of heat transfer increases with an increase in the radiation parameter. In the buoyancy-assisting flow region, the Sherwood number increases with increasing values of the radiation parameter, whereas, the opposite behavior is observed in the buoyancy-opposing flow region.
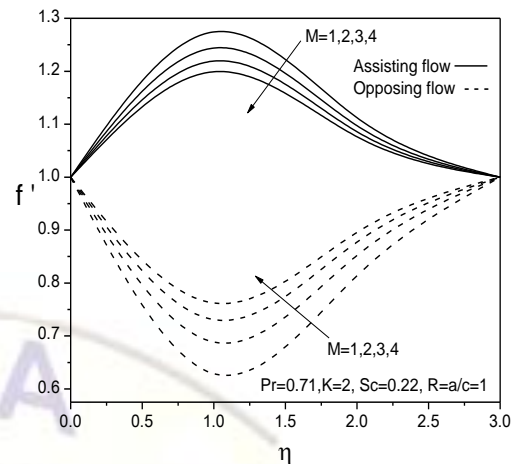
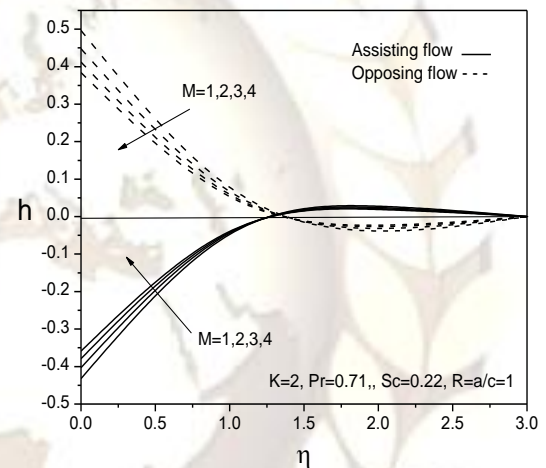Fig.1 Velocity profiles for different M
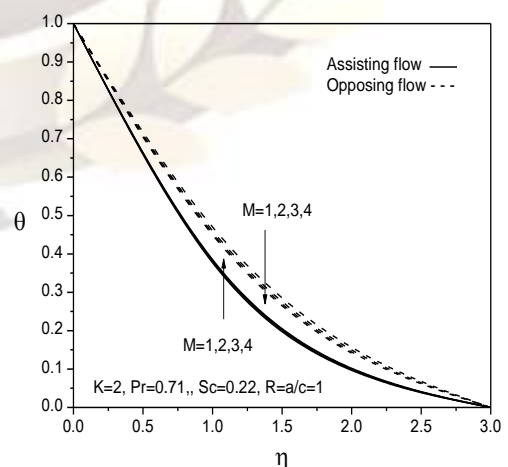

Fig.2 Microrotation profiles for different M

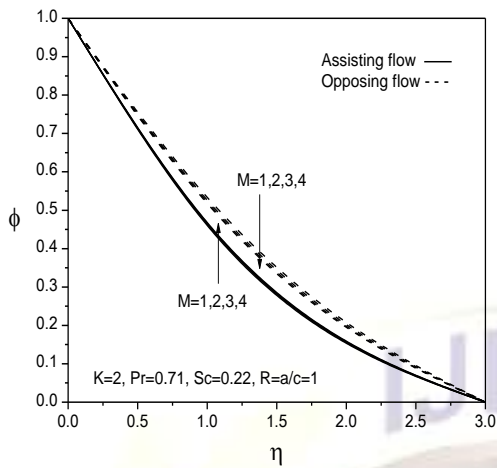Fig.3 Temperature profiles   for different M

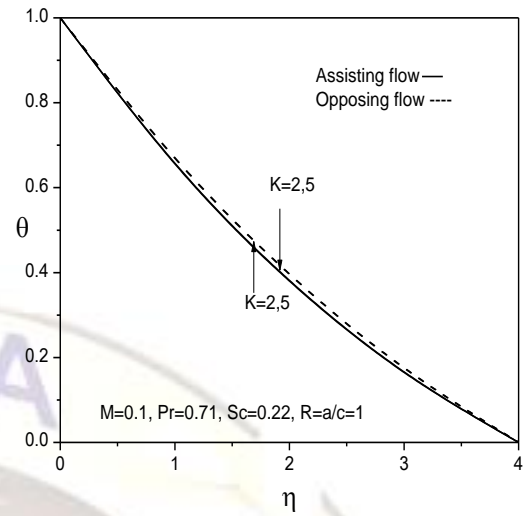Fig.4 Concentration profiles for different *M*

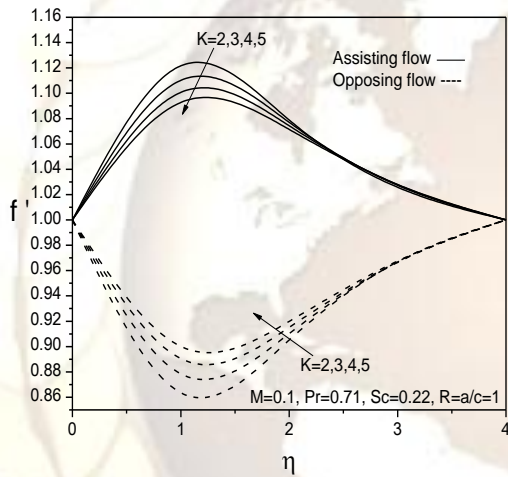Fig.7 Temperature profiles for different *K*

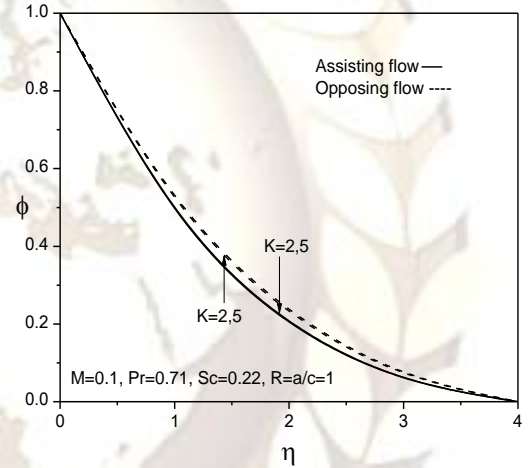Fig.5 Velocity profiles for different *K*

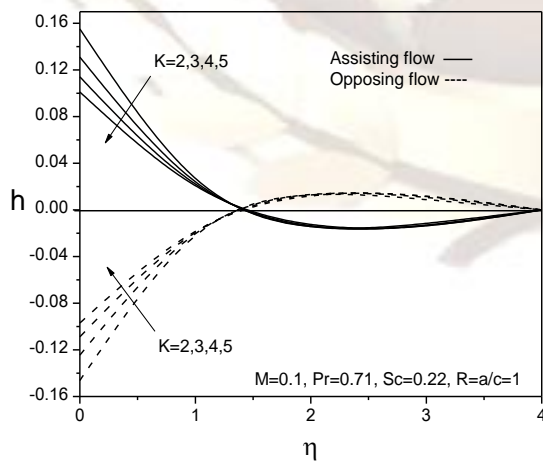Fig.8 Concentration profiles for different *K*
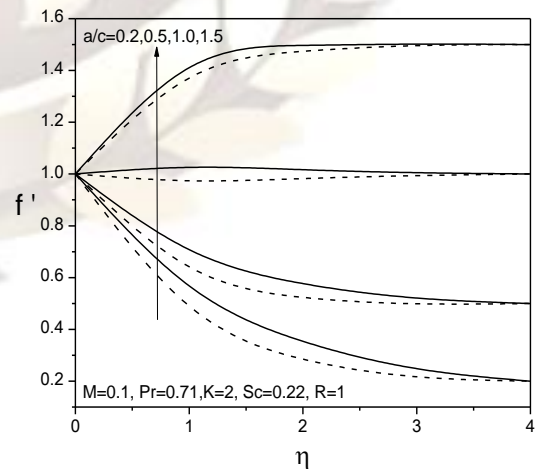

Fig.6 Microrotation profiles for different

K

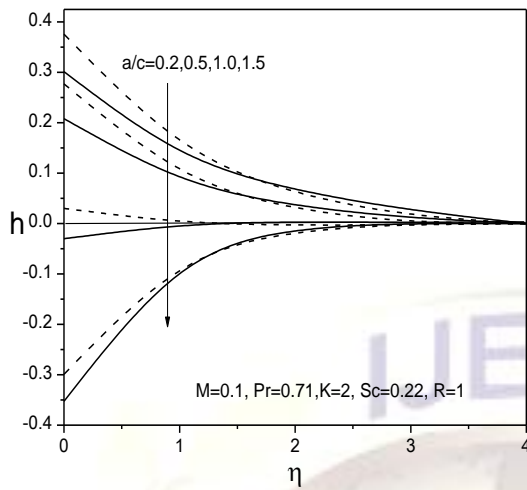Fig.9 Velocity profiles for different a/c

Fig.10 Microrotation profiles for different a/c

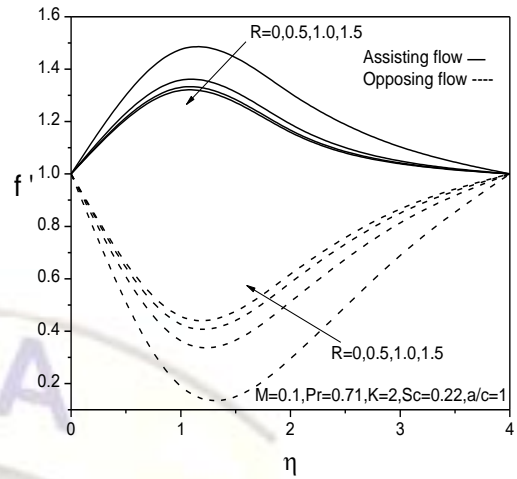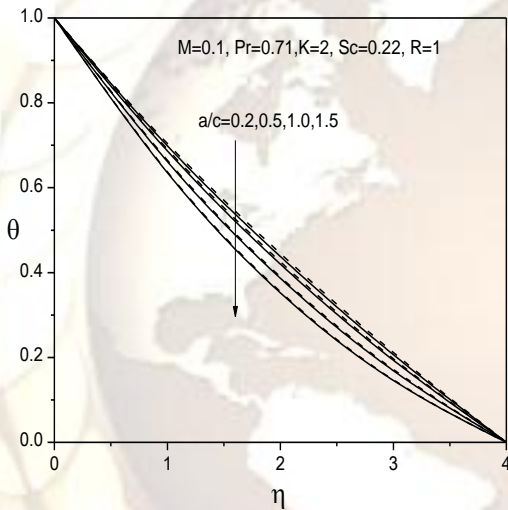Fig.13 Velocity profiles for different *R*
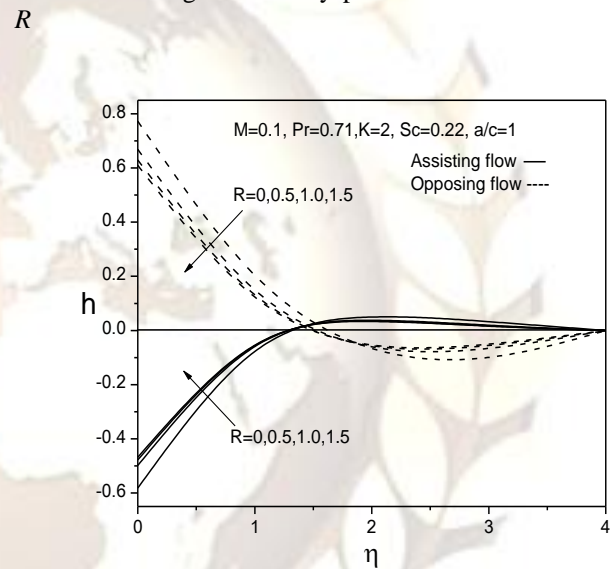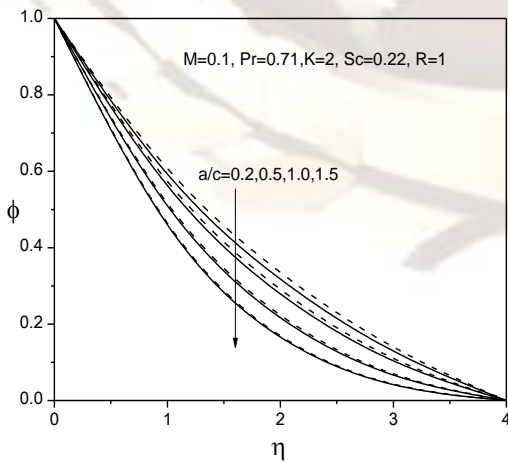

Fig.11 Temperature profiles for different a/c

Fig.14 Microrotation profiles for different *R*
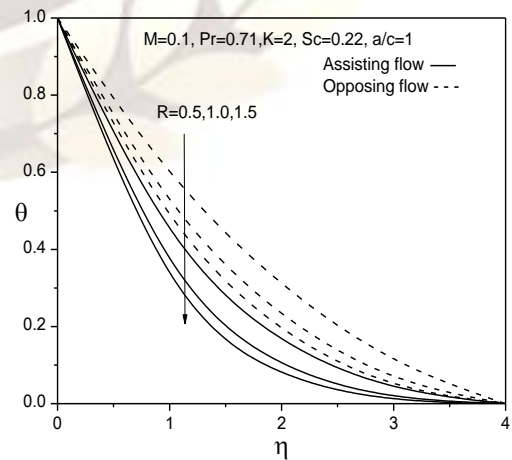

Fig.12 Concentration profiles for different a/c

Fig.15 Temperature profiles for different *R*
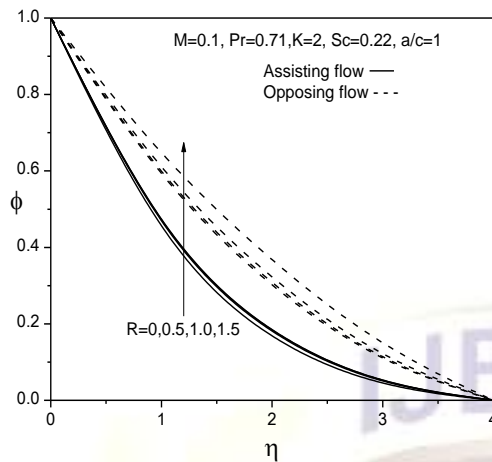
Fig.16 Concentration profiles for different *R*
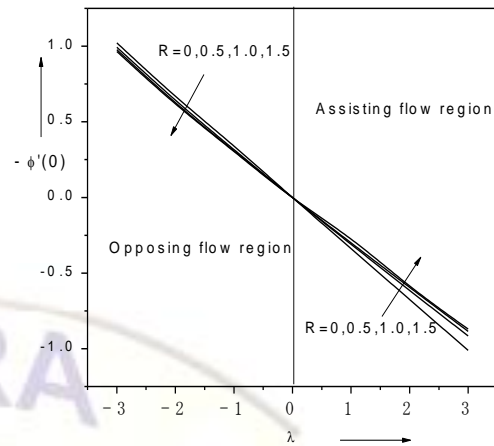
Fig.17   skin friction for different *R* (*M=0.1,   K=2,   λ=δ   a/c=1*)
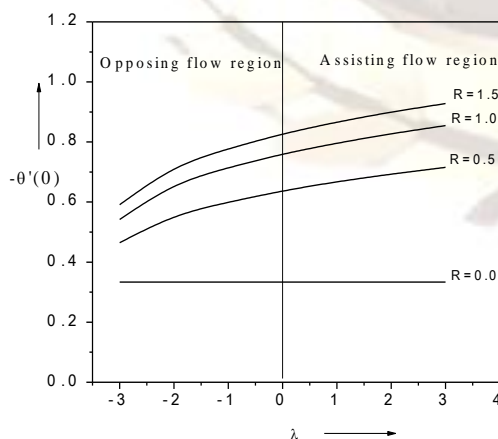
Fig.18 Nusselt number for different *R*

Fig.19 Sherwood number for different *R* (*M=0.1, K=2, λ=δ a/c=1*)

REFERENCES

[1]   Eringen, A. C., (1966), Theory of micropolar fluids, *Journal of Mathematics and Mechanics*, Vol.16, pp. 1-18.

[2]   Na, T. Y. and Pop, I., (1997), Boundary-layer flow of micropolar fluid due to a stretching wall, *Archives of Applied Mechanics*, Vol.67, No.4, pp. 229-236.

[3]   Desseaux, A. and Kelson, N. A., (2000), Flow of a micropolar fluid bounded by a stretching sheet, *Anziam J.*, Vol.42, pp.536-560.

[4]   Hady, F. M., (1966), on the solution of heat transfer to micropolar fluid from a non-isothermal stretching sheet with injection, *International Journal of Numerical Methods for Heat and Fluid Flow*, Vol.6, No.6, pp. 99-104.

[5]   Abo-Eldahab, E. M., and Ghonaim, A. F., (2003), Convective heat transfer in an electrically conducting micropolar fluid at a stretching surface with uniform free stream, *Appl. Math. Comput.*, Vol.137, pp. 323-336.

[6]   Mohammadein, A. A., and Gorla, R. S. R., (1998), Effects of transverse magnetic field on mixed convection in a micropolar fluid on a horizontal plate with vectored mass transfer, *Acta Mechanica*, Vol.118, pp.1-12.

[7]   Bhargava, R., Kumar, L., and Takhar, H.S., (2003b), Numerical solution of free convection MHD micropolar fluid flow between two parallel porous vertical plates, *Int. J. Engng Sci.*, Vol.41, pp. 123-136.

[8]   Srinivasacharya, D., and Shiferaw, M., (2008), Numerical solution to the MHD flow of micropolar fluid between two

concentric porous cylinders, *Int. J. of Appl. Math and Mech*., Vol.4, No.2, pp. 77-86.

[9] Rawat, S., Bhargava, R. and Anwar Bég, O., (2010), Hydromagnetic micropolar free convection heat and mass transfer in a darcy-forchheimer porous medium with thermophysical effects: finite element solutions, *Int. J. of Appl. Math and Mech*., Vol.6, No.13, pp. 72-93.

[10] Paullet, J. and Weidman, P., (2007), Analysis of stagnation point flow toward a stretching sheet, *International Journal of Non-Linear Mechanics*, Vol. 42, pp.1084–1091.

[11] Ishak, A., Nazar, R. and Pop, I., (2008b), Magnetohydrodynamic (MHD) flow of a micropolar fluid towards a stagnation point on a vertical surface". *Comp. Math. Appls*., Vol.56, pp.3188–3194.

[12] Lokendra Kumar, Singh B., Lokesh Kumar and Bhargava, R., (2011), Finite Element Solution of MHD Flow of Micropolar Fluid Towards a Stagnation Point on a vertical stretching sheet, *Int. J. of Appl. Math and Mech*., Vol.7, No.3, pp.14-30.

[13] Ishak, A., Nazar, R. and Pop, I., (2006), Mixed convection boundary layers in the stagnation-point flow toward a stretching vertical sheet. *Meccanica*, Vol.41, pp. 509–518.

[14] Ishak, A., Nazar, R. and Pop, I., (2008a), Mixed convection stagnation point flow of a micropolar fluid towards a stretching sheet, *Meccanica*, Vol.43, pp.411-418.

[15] Hassanien, I.A. and Gorla, R.S.R., (1990), combined forced and free convection in stagnation flows of micropolar fluids over vertical non-isothermal surfaces, *Int. J. Engng Sci*., Vol.28, pp. 783-792.

[16] Lok, Y.Y., Amin, N. and Pop, I., (2006), Unsteady mixed convection flow of a micropolar fluid near the stagnation point on a vertical surface, *Int. J. Therm.Sci*., Vol.45, pp.1149-1157.

[17] Bhargava, R., Kumar, L. and Takhar, H.S., (2003a), Finite element solution of mixed convection micropolar flow driven by a porous stretching sheet, *Int. J. Engng Sci*., Vol.41, pp. 2161-2178.

[18] Ogulu, A., (2005), On the oscillating plate-temperature flow of a polar fluid past a vertical porous plate in the presence of couple stresses and radiation, *Int. comm. Heat Mass Transfer*, Vol.32, pp. 1231–1243.

[19] Rahman, M.M. and Sattar, M.A., (2007), Transient convective flow of micropolar fluid past a continuously moving vertical porous plate in the presence of radiation, *Int. J. App. Mech. Engi*., Vol.12, No.2, pp.497–513.

[20] Abd-El Aziz, M. and Cairo, (2006), Thermal radiation effects on magnetohydrodynamic mixed convection flow of a micropolar fluid past a continuously moving semi-infinite plate for high temperature differences, *Acta Mechanica*, Vol.187, pp.113–127.

[21] Rahman, M.M. and Sultana, T., (2008), Radiative Heat Transfer Flow of Micropolar Fluid with Variable Heat Flux in a Porous Medium, *Nonlinear Analysis: Modelling and Control*, Vol. 13, No. 1, pp.71–87

[22] Callahan G.D. and Marner, W.J., (1976), Transient free convection with mass transfer on an isothermal vertical flat plate, *Int. J. Heat Mass Transfer*, Vol.19, pp.165-174.

[23] Soundalgekar, V.M. and Wavre, P. D., (1977), Unstedy free convection flow past an infinite vertical plate with constant suction and mass transfer, *Int. J. Heat Mass Trasfer*, Vol.20, pp.1363-1373.

[24] Kumar, L., (2009), Finite element analysis of combined heat and mass transfer in hydromagnetic micropolar flow along a stretching sheet. Comp. *Mater. Sci*., 46, pp. 841-848.

[25] Bhargava, R., Sharma S, Takhar, H.S., Bég, O. A. and Bhargava, P., (2007), Numerical solutions for micropolar transport phenomena over a nonlinear stretching sheet, *Nonlinear Analyis: Modelling and Control*, Vol.12, pp. 45–63.

[26] Brewster, M.Q., (1992), Thermal radiative transfer and properties, *John Wiley & sons. Inc.,* New York.

[27] Jain, M.K., Iyengar, S.R.K. and Jain, R.K., (1985), Numerical Methods for Scientific and Engineering Computation, *Wiley Eastern Ltd*., New Delhi, India.